Multiresolution texture analysis for human oocyte cytoplasm description

Article · May 2009

DOI: 10.1109/MEMEA.2009.5167974

4 authors, including:

Laura Caponetti
Università degli Studi di Bari Aldo Moro
62 PUBLICATIONS **415** CITATIONS
SEE PROFILE

Giovanna Castellano
Università degli Studi di Bari Aldo Moro
293 PUBLICATIONS **2,764** CITATIONS
SEE PROFILE

Vito Corsini
Politecnico di Bari
4 PUBLICATIONS **66** CITATIONS
SEE PROFILE

MeMeA 2009 - International Workshop on Medical Measurements and Applications
Cetraro, Italy
May 29-30, 2009

Multiresolution Texture Analysis for Human Oocyte Cytoplasm Description

Laura Caponetti*, Giovanna Castellano*, Vito Corsini†, Gianluca Sforza*
*Dipartimento di Informatica, Università degli Studi di Bari, via Orabona 4, 70100 Bari – Italia
Email: {caponetti, castellano, gsforza}@di.uniba.it
†Politecnico di Bari, via Orabona 4, 70100 Bari – Italia. Email: corsini@poliba.it

***Abstract*—In this work we present an approach based on image texture analysis to obtain a description of oocyte cytoplasm which could aid the medical expert in the selection of oocytes to be used for assisted insemination. More specifically, we describe some characteristics such as different levels of uniformity and/or granularity in the oocyte cytoplasm, using multiresolution texture analysis applied to light microscope images. To this aim, we evaluate some statistical measures in the wavelet transform domain of image regions and classify them according to different levels of granularity. Preliminary experimental results on a collection of light microscope images of oocytes are reported to show the effectiveness of the proposed approach.**

I. Introduction

A widely accepted view in the field of *Assisted Reproductive Technologies* is that viable embryos are a result of good quality gametes. While both the female and male gametes are equally important in the overall reproductive process, the oocyte plays a more fundamental role in hosting fertilization and embryogenesis.

There are currently some recognized morphological criteria by which oocytes are selected, including gross cytoplasmatic dysmorphisms – such as *granularity* and the presence of vacuoles –, *oolemma* elasticity, and oocyte size. Many other parameters have also been analysed in oocytes, such as *zona pellucida* thickness, *spindle birefrigence* and extracellular dysmorphisms [1]-[3]. In [4] a standardized procedure for the morphological assessment of *metaphase-II human oocytes* prior to ICSI (*Intra Cytoplasmic Sperm Injection*) is proposed, which is useful in selecting oocytes for insemination. Such procedure is based on the observation that human metaphase-II oocytes have distinct morphological characteristics that may be indicative of quality; for example, regular patterns of granularity have been observed in the oocyte cytoplasm, and it has been suggested that these patterns are related to oocyte quality [5]-[10].

In the last years, researchers have attempted to duplicate the human ability to understand the content of medical and biological images by developing image understanding algorithms able to interpret shape and texture of the observed images, and to assist medical analysis and diagnosis (e.g., [11]).

In this work we address the problem of automatically describing the cytoplasm of human oocytes, in order to evaluate their quality for ICSI. More specifically, our approach is intended to describe characteristics such as different levels of uniformity and/or granularity in oocyte cytoplasm, using multiresolution texture analysis applied to light microscope images (an example of such images is given in fig. 1). To this aim, we evaluate some statistical measures in the wavelet transform domain of image regions obtained after a preprocessing phase. A problem to be addressed is which levels of the wavelet transform should be used in the texture description. According to the work of Arivazhagan & Ganesan [12], our approach is based on the application of some statistical measures to the *approximation* and the *detail* regions resulting from a three-level *discrete wavelet transform* (DWT) of the original image.

The derived features describing oocyte images are then employed in a clustering phase in order to find a classification of oocytes according to their level of granularity. This is accomplished by applying the well-known Fuzzy C-means clustering algorithm.

The paper is organized as follows. In section II we describe all steps involved in the preprocessing phase of oocyte images. Section III details the texture analysis performed on preprocessed images, while Section IV gives a brief formalization of the fuzzy clustering algorithm. Finally, in section V some preliminary experimental results are provided to show the effectiveness of the proposed approach and some conclusions are drawn in Section VI.

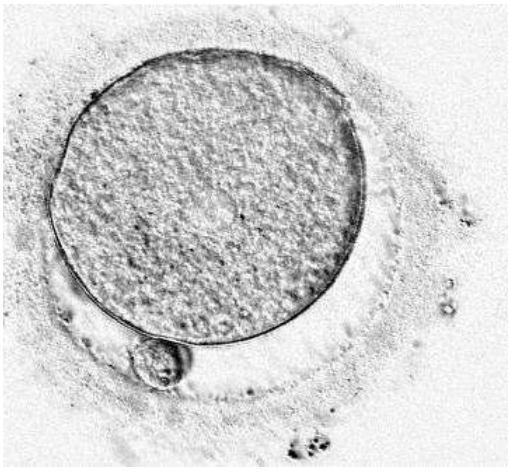

Fig. 1. Light microscope image of an oocyte with medium granularity

978-1-4244-3599-9/09/$25.00 ©2009 IEEE

II. Preprocessing

The preprocessing phase is devoted to automatically extract a region inside the oocyte cytoplasm to be used for the subsequent multiresolution texture analysis. This problem can be solved using image segmentation methods to detect different regions in the image. In past years, many methods for the segmentation of medical image have been presented [13], [14]. These methods include region-based methods, threshold based methods, and so on. The problem with these methods is that they employ only local information and do not consider a priori knowledge of object or region shape, such as area, radius or circumference. More recently in [15], [16], [17], image segmentation algorithms have been introduced, that combine a priori knowledge about structure and properties of objects with information contained in the image.

According to these last works, we segment the oocyte image by considering that the shape of the cytoplasm can be approximated by a circumference. Our method consists of the following steps: (1) obtain the gradient image; (2) use the gradient image to obtain points which possibly belong to circumference of different radius; (3) select the circumference that better approximates the cytoplasm boundary.

In the step (2) we use the Hough transform to obtain image points belonging to different circles. The Hough transform [18] is a powerful technique which can be used to isolate features of a particular shape in an image: it is most commonly used for the detection of regular curves such as lines, circles, ellipses, etc. The main advantage of the Hough transform is that it is tolerant of gaps in curve descriptions and is relatively unaffected by image noise.

The parameter space of the Hough transform is three-dimensional. Indeed, a circle with radius R and center (a, b) can be described by the following parametric equations:

$$x = a + R\cos(\theta),$$
$$y = b + R\sin(\theta).$$

When the angle θ sweeps through the full 360 degree range, the points (x, y) trace a circle of fixed radius R. The fact that the parameter space is three-dimensional makes a direct implementation of the Hough transform very expensive in terms of computer memory and time. Anyway, if the radius of circles in an image is known, then the parameter space can be reduced from 3D to 2D, thus the problem is reduced to searching for the coordinates (a, b) of the centers. Figure 2 shows the result of applying the Hough transform to the image in figure 3. In this last figure the circle that best fit to the cytoplasm boundary is overlapped on the original image.

Once the cytoplasm boundary is detected, we automatically select the region of interest by considering a rectangular region centered in the point of coordinates (a, b). This region is successively used for texture analysis, as described in the next section.

III. Texture analysis

According to [19], textures are complex visual patterns composed of entities, or subpatterns, that have characteristic brightness, color, slope, size, and scale. These properties give rise to the perceived lightness, uniformity, coarseness, smoothness, granularity of the image texture as a whole.

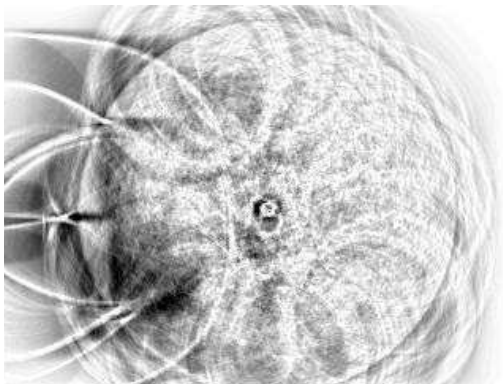

Fig. 2. Hough transform of an oocyte image

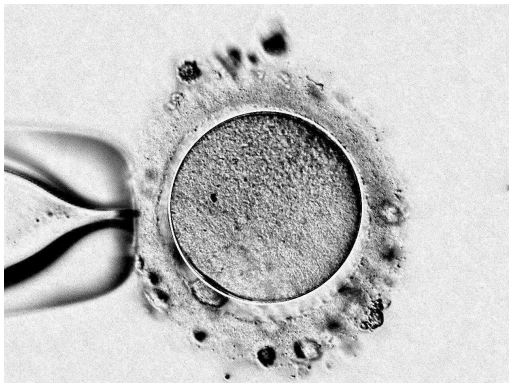

Fig. 3. Best fitting circle - plotted in white - overlapped on the oocyte image

A major class of texture descriptors relies on the assumption that texture can be defined by local statistical properties of pixel gray levels [20]. From the image histogram, first order statistics can be derived and used as texture measures.

Moreover a fundamental property of the image texture is the scale at which the image is observed and analyzed. For this reason several multiscale texture analysis approaches have been introduced [21], [22]. From these, wavelet theory has emerged as a formal, solid and unified framework for multiscale image analysis [23], [24]. The wavelet transform maps an image on a low resolution image and a series of detail images. The low resolution image is obtained by iteratively blurring the image itself; the detail images contain the information lost during this operation. The discrete wavelet transform can be computed by a cascade of high and low pass filtering followed by a factor 2 subsampling, applied first row by row and then column by column. For example at the first level of decomposition four subband images (labeled LL, HL, HH, LH in fig. 4), are obtained from the image with full resolution. To compute the successive level of decomposition, the process is iterated by applying the filtering and subsamplig

in the same way to the subband image LL.

To perform texture analysis, we use first order statistics applied to the multiresolution decomposition of the image. More specifically we characterize the texture with the following statistical properties of its multiscale representation:

1) mean;
2) variance, useful to establish descriptors of contrast;
3) a measure of relative smoothness;
4) third moment, that is a measure of the symmetry of the histogram;
5) a measure of uniformity, maximum for an image with all gray levels equal;
6) a measure of average entropy, that equals to 0 for a constant image.

These features, described in details in the Appendix, are computed on the histograms of the subband images obtained by the wavelet decomposition.

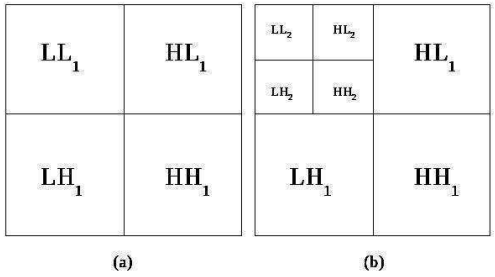

Fig. 4. Image decomposition. (a) One-level, (b) two level.

IV. Fuzzy clustering

Once a collection of feature vectors $\mathbf{x}_i, i = 1, ..., n$ describing oocyte images have been derived, a clustering process is applied in order to classify images according to their granularity. Each class will include images exhibiting a similar level of granulation. In this work, the well-known Fuzzy C-Means (FCM) clustering algorithm [25] is applied in order to group feature vectors $\mathbf{x}_i$ in overlapping clusters which represent classes. Briefly, the FCM algorithm finds *C* clusters based on the minimization of the following objective function:

$$F_m = \sum_{i=1}^{n}\sum_{c=1}^{C} u_{ic}^m \parallel \mathbf{x}_i - \mathbf{v}_c \parallel^2,$$

where m indicates the "fuzziness" of clustering (with higher values of m the boundaries between clusters become softer, with lower values they get harder), u_{ic} is the degree of membership of the feature vector $\mathbf{x}_i$ to the *c*-th cluster, $\mathbf{v}_c$ is the center of the *c*-th cluster. The FCM algorithm works as follows:

1) $\mathbf{U} = [u_{ic}]_{i=1,...,n}^{c=1,...,C}$ matrix, $\mathbf{U}^{(0)}$.
2) At τ-th step: calculate the center vectors $\mathbf{V}^{(\tau)} = (\mathbf{v}_c)_{c=1,...,C}$ as

$$\mathbf{v}_c = \frac{\sum_{i=1}^{n} u_{ic}^m \mathbf{x}_i}{\sum_{i=1}^{n} u_{ic}^m}.$$

3) Update $\mathbf{U}^{(\tau)}$ according to:

$$u_{ic} = \frac{1}{\sum_{k=1}^{C} (\frac{\|\mathbf{x}_i - \mathbf{v}_c\|}{\|\mathbf{x}_i - \mathbf{v}_k\|})^{\frac{2}{m-1}}}.$$

4) Return to step 2 while the condition $\parallel \mathbf{U}^{(\tau)} - \mathbf{U}^{(\tau-1)} \parallel \leq \epsilon$ is verified, where ϵ is a user-specified parameter.

As a result, FCM provides:

- C cluster prototypes represented as vectors $\mathbf{v}_c = (v_{c1}, v_{c2}, ..., v_{cm})$ for $c = 1, ..., C$.
- a fuzzy partition matrix $\mathbf{U} = [u_{ic}]_{i=1...n}^{c=1...C}$ where u_{ic} represents the membership degree of the feature vector $\mathbf{x}_i$ to the *c*-th cluster.

Summarizing, the FCM mines a collection of C clusters representing classes of similar oocyte images. Each prototype $\mathbf{v}_c = (v_{c1}, v_{c2}, ..., v_{cm})$ describes the features of a group of images having a similar level of granularity.

V. Experimental results and discussion

The proposed approach was tested on 60 light microscope images of human oocytes, provided by the *Dipartimento di Endocrinologia ed Oncologia Molecolare e Clinica* of the University "Federico II" of Naples, Italy. Each image was large 1280x960 pixels.

Firstly, each image was preprocessed using the Hough transform, so as to detect the best circle fitting the real shape of the oocyte cytoplasm. This was done by searching circles of known radius R ranging from 230 to 250 pixels. Once the circular region of the cytoplasm was identified, a squared region of 128x128 pixels centered in the circular region was extracted. All steps involved in the preprocessing phase were implemented using *ImageJ*, a public domain Java image processing tool available either as an online applet or as a downloadable application at `http://rsbweb.nih.gov/ij/`.

Then, we applied the texture analysis on each squared region by employing a three-level *Haar wavelet transform*. After an investigation of the statistical distributions of the selected features (i.e., mean, variance, relative smoothness, third moment, uniformity, and entropy), calculated for each level of the DWT coefficients, we observed that distributions at the second and at the third level have a quite similar trend. Therefore, we decided to retain only features calculated for the coefficients of a two-level wavelet transform. Namely, we applied a two-level DWT to each texture region, generating six detail and one approximation subband regions. Over these subbands, the six selected features were computed to describe their histogram. To implement texture analysis methods, some Java plugins were developed and properly integrated into the ImageJ environment.

Next, the FCM algorithm (implemented in the *Matlab* environment 6.5) was applied on the derived feature vectors in order to find a classification of the oocyte cytoplasm

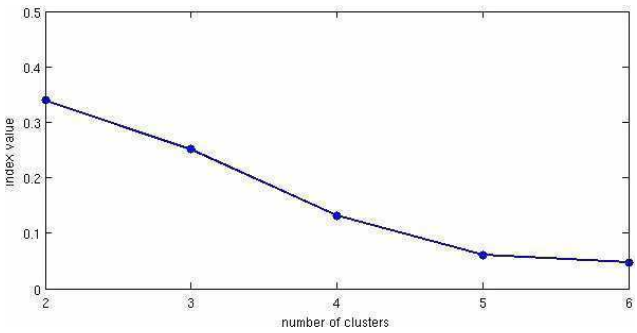

Fig. 5. Dunn index for different FCM clustering

images. Before applying FCM, all the considered features were normalized. The FCM was run with $m = 2$, a standard value that we found experimentally to provide the best minimization of the objective function.

Several runs of the FCM were carried out, corresponding to a number of clusters C ranging from 2 to 6. For each run, we evaluated the quality of the clustering result by means of the Dunn index [26], defined as follows:

$$D = \min_{1\le i\le C}\left\{\min_{1\le j\le C}\left\{\frac{\delta(X_i, X_j)}{\max_{1\le k\le C}\{\Delta(X_k)\}}\right\}\right\},$$

where $\delta(X_i, X_j)$ represents the *intercluster distance* between clusters X_i and X_j, $\Delta(X_k)$ represents the *intracluster distance* of cluster X_k and C is the number of clusters. Typically, the goal of clustering is to maximize intercluster distances whilst minimizing intracluster distances. Hence, large values of Dunn's index correspond to a better clustering result.

Figure 5 plots the values of the Dunn index obtained by applying FCM with different number of clusters.

It can be seen that better values are obtained for $C = 2$ and $C = 3$, while the results are worsen for higher values of C. This suggested to retain only the results obtained with two and three clusters as acceptable classification of the considered images. However, after a visual inspection of the generated clusters, we found that with $C = 2$ the derived classes are quite crowded and very difficult to interpret. Conversely, classes identified with $C = 3$ resembled a classification made by a human expert. Specifically, the three obtained clusters provided the following classification of oocyte images:

- cluster 1: Oocytes with medium/high granularity and eventually some anomalies such as inclusions or vacuoles (25% of the total number of oocytes);
- cluster 2: Oocytes with medium granularity (40% of the total number of oocytes);
- cluster 3: Oocytes with low granularity (35% of the total number of oocytes);

As an example, figure 6 shows six image regions belonging to each of the three cluster. It can be seen that regions belonging to cluster 1 (first row) have a quite high level of granularity, regions belonging to cluster 2 (second row) share a medium level of granularity and sometimes present anomalies, while regions belonging to cluster 3 are weakly granulated. A qualitative analysis of these clustered regions made by a medical expert confirmed that they correspond to a good classification of the oocytes.

VI. Conclusions

In this paper an approach for the description and classification of human oocyte cytoplasm using multiresolution texture analysis has been proposed. Preliminary experimental results on real oocyte images show the effectiveness of the approach and encourage its application in the process of assessing the quality of human oocytes. In particular, the work presented in this paper is intended as a preliminary step toward the development of a computer-based second opinion diagnostic tool for the morphological scoring of human oocytes. This system will be able to analyze microscope images of human oocytes and classify them as "top quality" or "low scoring" oocytes during ICSI cycles. Currently, further work is in progress to complete the development of such diagnostic tool.

Appendix

Let u be a random variable representing a gray-level in a given region of the image, and L the number of gray levels. The histogram is defined as a mapping $p_u : \{0, \dots, L-1\} \to [0, 1]$ where

$$p_u(x) \stackrel{\text{def}}{=} Prob[u = x] \quad \simeq \quad \frac{\text{no. of pixels with gray level } x}{\text{total no. of pixels in the region}}, \qquad x = 0, \dots, L-1. \tag{1}$$

Common features of $p_u(x)$ are its moments, which are defined next.

$$\text{Moments:} \quad m_i = \sum_{x=0}^{L-1} x^i p_u(x), \tag{2}$$

$$\text{Central moments:} \quad \mu_i = \sum_{x=0}^{L-1} (x - m_1)^i p_u(x), \qquad i = 1, 2, \dots. \tag{3}$$

From Eq.(2), the first moment m_1 is the average gray level, i.e., *the mean*, that is useful only as a rough idea of intensity. The second central moment μ_2 is the $variance$, particularly important in texture description. It is a measure of gray-level contrast that can be used to establish descriptors of *relative smoothness*, such as the measure

$$R = 1 - \frac{1}{1 + \mu_2(u)}. \tag{4}$$

The value of R is 0 for areas of constant intensity(smooth areas), and approaches to 1 for large values of $\mu_2(u)$ (coarse areas). The third moment, $\mu_3(u)$, is a measure of the simmetry of the histogram, so determining its relative skewness: negative values state for left-skewed histograms, while positive values determine the right ones. This gives an idea of whether the gray levels are biased toward the dark or light side of the mean.

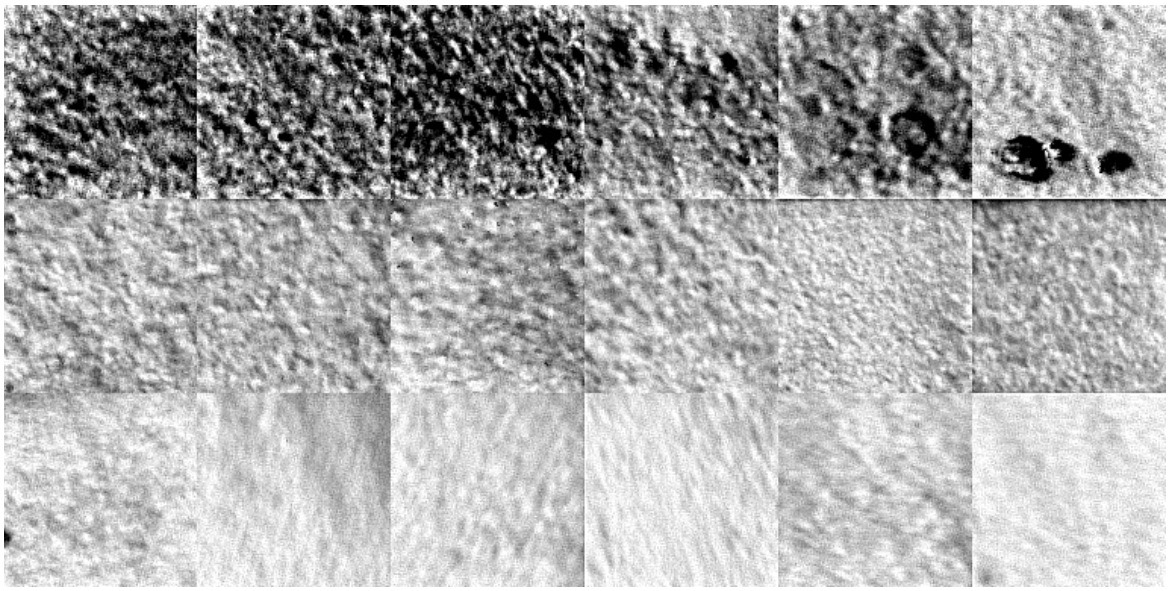

Fig. 6. Classification of oocyte image regions obtained by FCM clustering. First, second and third row represents regions belonging to cluster 1, 2 and 3, respectively.

Some useful additional texture features based on histograms include a measure of *uniformity,* given by

$$U = \sum_{x=0}^{L-1} p_u^2(x), \tag{5}$$

that is maximum for an image in which all gray levels are equal, and an *average entropy* measure, which is defined as

$$E = -\sum_{x=0}^{L-1} p_u(x) \log_2 p_u(x) \text{ bits}, \tag{6}$$

that equals to 0 for a constant image.

ACKNOWLEDGMENT

This work was supported by the italian project *MIUR-FAR 08-09: Laboratorio di Bioinformatica per la Biodiversitá Molecolare (MBLab-DM19410).*

REFERENCES

[1] P. de Sutter, D. Dozortsev, C. Qian, and M. Dhont, "Oocyte morphology does not correlate with fertilization rate and embryo quality after intracytoplasmic sperm injection," *Human Reproducion*, no. 11, pp. 595–597, 1996.

[2] M. Alikani *et al.*, "Intracytoplasmic sperm injection in dysmorphic human oocytes," *Zygote*, no. 3, pp. 283–288, 1995.

[3] Y. Shen *et al.*, "Light retardance by human oocyte spindle is positively related to pronuclear score after icsi," *Reproductive Bio Medicine Online*, no. 12, pp. 737–751, 2006.

[4] M. Wilding *et al.*, "An oocyte score for use in assisted reproduction," *Journal of Assisted Reproduction and Genetics*, vol. 24, no. 8, pp. 350–358, 2007.

[5] S. Hamamah, "Oocyte and embryo quality: is their morphology a good criterion?" *Journal of Obstetrics & Gynecology and Reproductive Biology*, no. 34, pp. 5S38–5S41, 2005.

[6] P. Serhal *et al.*, "Oocyte morphology predicts outcome of intracytoplasmic sperm injection," *Human Reproducion*, no. 12, pp. 1267–1270, 1997.

[7] D. Loutradis *et al.*, "Oocyte morphology correlates with embryo quality and pregnancy rate after intracytoplasmic sperm injection," *Fertility and Sterility*, no. 72, pp. 240–244, 1999.

[8] S. Suppinyopong, R. Choavaratana, and C. Karavakul, "Correlation of oocyte morphology with fertilization rate and embryo quality after intracytoplasmic sperm injection," *Journal of The Medical Association of Thailand*, no. 83, pp. 627–632, 2000.

[9] M. Plachot *et al.*, "Consequences of oocyte dysmorphy on the fertilization rate and embryo development after intracytoplasmic sperm injection. a prospective multicenter study," *Gynecology Obstetrique & Fertilite*, no. 30, pp. 772–779, 2002.

[10] T. Stalf *et al.*, "Influence of polarization effects in ooplasma and pronuclei on embryo quality and implantation in an ivf program," *Journal of Assisted Reproduction and Genetics*, no. 19, pp. 355–362, 2002.

[11] L. Kaplan, "Extended fractal analysis for texture classication and segmentation," *IEEE Transactions on Image Processing*, vol. 8, no. 11, pp. 1572–1585, 1999.

[12] S. Arivazhagan and L. Ganesan, "Texture classification using wavelet transform," *Pattern recognition letters*, no. 24, pp. 1513–1521, 2003.

[13] C. Garbay, "Image structure representation and processing discussion of some segmentation methods in cytology," *IEEE Trans. Pattern Anal. Mach. Intell.*, vol. 8, no. 2, pp. 140–146, 1986.

[14] H.-S. Wu, J. Barba, and J. Gil, "Iterative thresholding for segmentation of cells from noisy images," *Journal of Microscopy*, vol. 197, no. 3, pp. 296–304, 2000.

[15] ——, "A parametric fitting algorithm for segmentation of cell images," *Biomedical Engineering, IEEE Transactions on*, vol. 45, no. 3, pp. 400–407, March 1998.

[16] F. Yang and T. Jiang, "Cell image segmentation with kernel-based dynamic clustering and an ellipsoidal cell shape model," *Comput. Biomed. Res.*, vol. 34, no. 2, pp. 67–73, 2001.

[17] D. W. McKee, J. Walker H. Land, T. Zhukov, D. Song, and W. Qian, "An adaptive image segmentation process for the classification of lung biopsy images," J. M. Reinhardt and J. P. W. Pluim, Eds., vol. 6144, no. 1. SPIE, 2006, p. 614452. [Online]. Available: http://link.aip.org/link/?PSI/6144/614452/1

[18] J. Sklansky, "On the hough technique for curve detection," *IEEE Trans. Comput.*, vol. 27, no. 10, pp. 923–926, 1978.

[19] M. Levine, *Vision in Man and Machine*. McGraw-Hill, 1985.

[20] R. Gonzalez and R. Woods, *Digital Image Processing, 2nd ed.* Prentice Hall, 2001.

[21] M. Unser and M. Eden, "Multiresolution feature extraction and selection for texture segmentation," *IEEE Transactions on Pattern Analysis and Machine Intelligence*, vol. 11, no. 7, pp. 717–728, 1989.
[22] A. K. Jain and K. Karu, "Learning texture discrimination masks," *IEEE Transactions on Pattern Analysis and Machine Intelligence*, vol. 18, no. 2, pp. 195–205, 1996.
[23] S. Mallat, "A theory for multiresolution signal decomposition: The wavelet representation," *IEEE Transactions on Pattern Analysis and Machine Intelligence*, vol. 11, no. 7, pp. 674–693, 1989.
[24] I. Daubechies, *Ten Lectures on Wavelets*. Soc for Industrial & Applied Math, December 1992. [Online]. Available: http://www.amazon.ca/exec/obidos/redirect?tag=citeulike09-20&path=ASIN/0898712742
[25] J. C. Bezdek, *Pattern Recognition with Fuzzy Objective Function Algorithms*. Norwell, MA, USA: Kluwer Academic Publishers, 1981.
[26] M. Halkidi, Y. Batistakis, and M. Vazirgiannis, "Clustering validity checking methods: part ii," *SIGMOD Rec.*, vol. 31, no. 3, pp. 19–27, 2002.